Simulation and experimental verification of prompt gamma-ray emissions during proton irradiation

Schumann, A.; Petzoldt, J.; Dendooven, P.; Enghardt, W.; Golnik, C.; Hueso-Gonzalez, F.; Kormoll, T.; Pausch, G.; Roemer, K.; Fiedler, F.

Published in:
Physics in Medicine and Biology

DOI:
10.1088/0031-9155/60/10/4197

Publication date:
2015

PAPER

Simulation and experimental verification of prompt gamma-ray emissions during proton irradiation

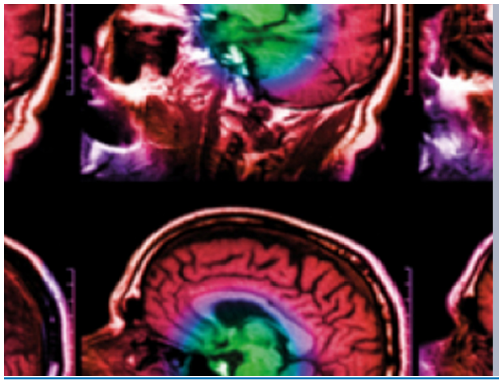

IOP Publishing | Institute of Physics and Engineering in Medicine Physics in Medicine & Biology

Phys. Med. Biol. **60** (2015) 4197–4207 doi:10.1088/0031-9155/60/10/4197

Simulation and experimental verification of prompt gamma-ray emissions during proton irradiation

A Schumann[1], J Petzoldt[2], P Dendooven[3], W Enghardt[2,4], C Golnik[2], F Hueso-González[4], T Kormoll[2], G Pausch[2], K Roemer[1] and F Fiedler[1]

[1] Helmholtz-Zentrum Dresden-Rossendorf, Institute of Radiation Physics, Bautzner Landstr. 400, 01328 Dresden, Germany
[2] OncoRay: National Center for Radiation Research in Oncology, Faculty of Medicine and Univeristy Hospital Carl Gustav Carus, Technische Universität Dresden, Fetscherstr. 74, PF 41, 01307 Dresden, Germany
[3] KVI: Center for Advanced Radiation Technology, University of Groningen, Zernikelaan 25, 9747 AA Groningen, The Netherlands
[4] Helmholtz-Zentrum Dresden-Rossendorf, Institute of Radiooncology, Bautzner Landstr. 400, 01328 Dresden, Germany

E-mail: a.schumann@hzdr.de

Received 24 November 2014, revised 6 March 2015
Accepted for publication 10 April 2015
Published 8 May 2015

Abstract

Irradiation with protons and light ions offers new possibilities for tumor therapy but has a strong need for novel imaging modalities for treatment verification. The development of new detector systems, which can provide an *in vivo* range assessment or dosimetry, requires an accurate knowledge of the secondary radiation field and reliable Monte Carlo simulations. This paper presents multiple measurements to characterize the prompt γ-ray emissions during proton irradiation and benchmarks the latest Geant4 code against the experimental findings. Within the scope of this work, the total photon yield for different target materials, the energy spectra as well as the γ-ray depth profile were assessed. Experiments were performed at the superconducting AGOR cyclotron at KVI-CART, University of Groningen. Properties of the γ-ray emissions were experimentally determined. The prompt γ-ray emissions were measured utilizing a conventional HPGe detector system (Clover) and quantitatively compared to simulations. With the selected physics list QGSP_BIC_HP, Geant4 strongly overestimates the photon yield in most cases, sometimes up to 50%. The shape of the spectrum and qualitative occurrence of discrete γ lines is reproduced accurately. A sliced phantom was designed to determine the depth profile of the photons. The position of

the distal fall-off in the simulations agrees with the measurements, albeit the peak height is also overestimated. Hence, Geant4 simulations of prompt γ-ray emissions from irradiation with protons are currently far less reliable as compared to simulations of the electromagnetic processes. Deviations from experimental findings were observed and quantified. Although there has been a constant improvement of Geant4 in the hadronic sector, there is still a gap to close.

Keywords: proton therapy, prompt gamma imaging, Geant4

(Some figures may appear in colour only in the online journal)

1. Introduction

Radiotherapy with protons and light ions offers significant advantages compared to conventional photon and electron-based tumor treatment. Nevertheless, reliable imaging and treatment verification techniques are still missing in the clinical routine. Numerous concepts of *in vivo* range verification possibilities during proton therapy exist (Knopf and Lomax 2013). Currently, particle therapy positron emission tomography (PT-PET) is the only clinically proven range verification modality (Paans and Schippers 1992, Enghardt *et al* 2004, Parodi *et al* 2007, Fiedler *et al* 2012). Still, due to the half-life of the positron emitters, it cannot be used in real-time, which limits its usability in the clinical workflow.

To overcome these limitations, range verification with prompt γ-rays was suggested (Min *et al* 2006). The nuclei within the patient tissue are excited during the slowing down process of the protons. De-excitation and emission of photons with energies up to several MeV take place on the order of picoseconds or even faster. Hence, biological wash-out can be neglected and it is possible to obtain real-time information. Nevertheless, new detector concepts are required to unlock the full potential which prompt γ-ray emissions might offer. Several detector systems are currently under investigation e.g. slit cameras for pure range verification measurements (Verburg *et al* 2013), Compton cameras which should be able to measure 3D γ-ray emission distributions for *in vivo* dosimetry (Kormoll *et al* 2011) or new approaches based on prompt γ timing (Golnik *et al* 2014).

Development of novel detector systems for prompt gamma imaging (PGI), requires a comprehensive understanding of the photon field which is produced during the proton irradiation and reliable Monte Carlo (MC) techniques to model these secondary particles. Within this work, multiple irradiations of several phantoms will be presented and an analysis of the total γ-ray yield, the energy spectra and depth distribution will be given. The main focus was on photons in the energy range from 3 MeV to 7 MeV, which are most promising for these imaging modalities. All experimental findings were compared to Geant4 MC simulations and their agreement was assessed.

2. Materials and methods

Experiments were performed at the superconducting cyclotron Accélérateur Groningen-Orsay (AGOR), situated at the KVI-Center for Advanced Radiation Technology (KVI-CART) facility at the University of Groningen, the Netherlands. The cave housing the AGOR Facility for Irradiation of Materials (AGORFIRM) beam-line was used for the setup (van der Graaf *et al* 2009). Multiple phantoms made of different materials were irradiated to evaluate the prompt

γ-ray yield, the energy spectrum and the depth gamma profile (DGP). MC simulations of the experimental setup with Geant4 were conducted for comparison with the measurements. This section describes the experimental setup and the Geant4 simulations in detail. Additionally, a short description of the assessment of the different errors for the γ-ray yield data will be given.

2.1. Experimental setup

The proton energy was fixed to 150 MeV. Protons exiting the cyclotron have an energy uncertainty of less than 0.25%. At this energy, the AGOR cyclotron operates with a radio frequency (RF) of 55 MHz.

The proton beam current was observed using the in-house beam-monitoring system. During its calibration, the beam current was lowered until the number of protons could be counted with a scintillation detector. The corresponding number of monitor units (MUs) from the ionization chamber was related to the number of protons. After calibration, the scintillation detector was removed. The gain of the ionization chamber signal amplifier can be changed very accurately in steps of factors of ten. The gain setting is decreased for higher beam currents in order to keep the MU count rate within the limits of the MU counting system. As such, because of the very accurately controlled gain of the ionization chamber signal, the calibration performed with very low beam current was valid for beam currents many orders of magnitude higher as used in the measurements.

The MUs were fed into a charge counter which was vetoed with the crate's busy signal. Real and live charge counts represented the applied MUs for each irradiation. Additionally, a frequency generator (time counter) was used to determine the dynamic system dead-time. This allowed an accurate dead-time correction for the whole experiment. Afterwards, the proton number n_p was calculated with

$$n_p = C \cdot N_c \tag{1}$$

where C is the calibration factor and N_c the live charge counter output. The relative errors from the measurement time and detector-target distance were $<10^{-3}$ and at least one order of magnitude smaller when compared to the error of the MU to proton number scaling.

For measuring the prompt γ-ray emissions, a high purity germanium (HPGe) detector, the so-called Clover, was used. The Clover is a composite semiconductor detector and consists of four separate n-type HPGe crystals, which are arranged like a four-leaf clover. It offers good energy resolution and can be operated in add-back mode to improve the photo-peak efficiency (Duchêne *et al* 1999, Elekes *et al* 2003). Extensive work was performed to incorporate the detector geometry into the MC simulations. The Clover was operated without anti-Compton shield and the crystals were read-out individually. Afterwards, the four channels were calibrated and the energy deposition was summed for every event (add-back mode). A sketch of the experimental setup is shown in figure 1.

At the position of the isocenter (57.5 cm behind the beam exit window), the Clover was placed at an angle of 90° to the beam axis. Several phantoms were irradiated throughout the experiment. They where positioned with the median of the expected (simulated) DGP at the isocenter. Full absorption measurements, where the proton beam was completely stopped, were conducted with blocks of polyethylene (PE), graphite and cortical bone equivalent material (SB3). SB3 consists of O (36.5%), C (31.4%), Ca (26.8%), H (3.4%) and N (1.8%) and was manufactured by the company Gammex. Additionally, seven measurements with polymethyl methacrylate (PMMA) phantoms of varying thickness were performed to assess the depth profile of the prompt γ-ray emissions. The so-called *sliced phantom* was built from several 1 cm and 3 cm PMMA slabs up to a total thickness of 15 cm. At this depth, total absorption

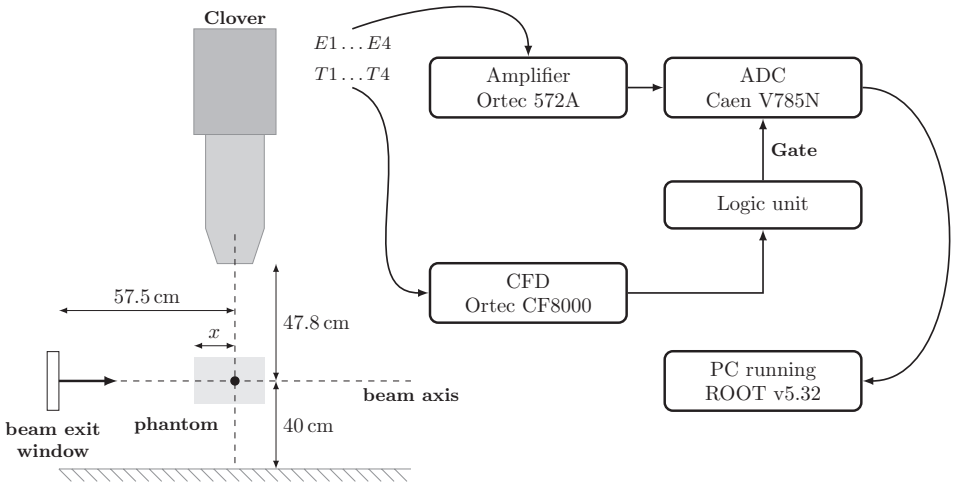

Figure 1. (Left) Experimental setup at the AGORFIRM beam-line. The sketch shows the Clover detector mounted in a 90° angle to the beam axis. The proton beam was coming from the left. The black dot at the intersection of the Clover central axis and the proton beam marks the isocenter. The distance (x) of the phantom's front-face to the isocenter varied, depending on the phantom material. (Right) Schematic view of the electronic setup. Every crystal had two outputs which were used to provide the ADC (E) and a gating signal (T) for the corresponding channels.

of 150 MeV protons in PMMA is achieved. The beam dump was about 410 cm behind the isocenter. During the measurements of thinner targets, the protons traversing the phantom and hitting the beam dump contribute to the overall signal. Applying the inverse square law, this contribution can be estimated to be less than 2%.

The following differential analysis of the measured photon yields was used to reconstruct the DGP in PMMA. The number of photons per proton per cm depth y_i for the ith slice can be written as:

$$y_i = \begin{cases} \dfrac{x_i}{s_i}, & i = 1 \\ \dfrac{x_i - x_{i-1}}{s_i}, & i > 1 \end{cases} \tag{2}$$

where x_i is the number of photons per protons in the ith measurement and s_i the thickness of the current slice. The total thickness of the PMMA phantom was increased from 5 cm to 15 cm resulting in seven measurements (see also table 1).

2.2. Monte Carlo simulations with Geant4

MC simulations were computed with Geant4 (Agostinelli *et al* 2003), release v10.00.p01 with the physics list QGSP_BIC_HP. Detailed information about this reference physics list is given subsequently and can be obtained from Geant4 user support web page[5]. The list is based on a parton or quark gluon string (QGS) model which describes high energy (12 GeV–100 TeV) hadronic interactions of protons, neutrons, π and K mesons. It also includes the precompound model (P). Reactions below 10 GeV are handled by the intranuclear cascade model Binary

[5] http://geant4.web.cern.ch/geant4/support/proc_mod_catalog/physics_lists/referencePL.shtml.

Table 1. Summary of the different measurements: the measurements lasted from about 12 min–30 min for the PMMA slices to over 70 min (PE target). For the *sliced phantom*, i denotes the measurement number and s_i the thickness of the added slice.

Target	i	s_i cm	Total thickness cm	Dead-time %	Time s
	1	5	5	23.6	1894
	2	3	8	31.1	1785
	3	3	11	33.4	1813
PMMA	4	1	12	35.1	699
	5	1	13	34.6	1773
	6	1	14	35.4	1795
	7	1	15	35.7	1791
PE			25	26.0	4362
Graphite			30	35.0	3718
SB3			12	36.5	2235

Note: The proton beam currents ranged from about 8.6–16.5 pA with a standard deviation within one measurement of less than 10%, except for the SB3 measurement.

cascade (BIC). Low energy final states of hadron inelastic scattering are generated by the pre-compound model which is valid below 170 MeV. The high precision neutron (HP) package provides data-driven neutron processes from 20 MeV down to thermal energies, i.e. Geant4 uses an evaluated neutron data library (G4NDL) for cross sections, angular distributions and final state information[6]. Proton dose calculation in Geant4 is already well-established since version 8.1. For this purpose, a combination of the BIC model for the nuclear and the standard electromagnetic (EM) models for the electronic interactions is recommended (Jarlskog and Paganetti 2008). The BIC model also offers improved nuclear de-excitation handling and is supposed to better describe production of secondary particles created in interactions of protons and neutrons with nuclei compared to parametrized models.

For photons, electrons and positrons the range cuts were fixed in all runs to 10 cm, while for protons they were set to 1 μm. In Geant4, the concept of production cuts is used to achieve a compromise between computation time and accuracy. From these range cuts, threshold energy are calculated for each particle type and material. A particle with this threshold energy is stopped or absorbed after traveling the range cut distance. In general and not considering certain exceptions, secondary particles which are created with kinetic energies below this threshold will not be tracked and the energy is deposited locally[7]. These thresholds effectively decrease the number of directly created and bremsstrahlung induced low energy photons. Since the main interest was attributed to γ-rays with energies above 2 MeV, this influence is negligible and the performance advantage was exploited.

The experimental setup, including the complex geometry of the Clover crystals and casing, were modeled and the different irradiations were simulated. This allows a quantitative comparison of the γ-ray yield measured in the experiment with the MC simulations.

2.3. Error analysis

In this section, the analysis of the different errors of experiment and simulation are described. The random error was calculated from the number of counts N:

[6] http://geant4.web.cern.ch/geant4/UserDocumentation/UsersGuides/PhysicsReferenceManual/fo/PhysicsReferenceManual.pdf.

[7] http://geant4.web.cern.ch/geant4/UserDocumentation/UsersGuides/ForApplicationDeveloper/html/index.html.

$$\Delta N = \sqrt{N} \tag{3}$$

The error of the number of protons was estimated from the MU to proton number conversion and according to (1) it was calculated as follows:

$$\frac{\Delta n_\mathrm{p}}{n_\mathrm{p}} = \frac{\Delta C}{C} + \underbrace{\frac{\Delta N_\mathrm{c}}{N_\mathrm{c}}}_{\ll \frac{\Delta C}{C}} \approx \frac{\Delta C}{C} \tag{4}$$

The relative error of the live charge counts N_c could be neglected, since it was about two orders of magnitude smaller than the error of the calibration factor C. The number of photons per proton x_i was calculated as follows:

$$x_i = \frac{N_\gamma}{n_\mathrm{p}} \quad \longrightarrow \quad \frac{\Delta x_i}{x_i} = \frac{\Delta n_\mathrm{p}}{n_\mathrm{p}} + \underbrace{\frac{\Delta N_\gamma}{N_\gamma}}_{\frac{1}{\sqrt{N_\gamma}}} \tag{5}$$

where N_γ is the number of photons in the specified energy interval. Except for the intervall from 3 MeV to 7 MeV the continuous background was subtracted using a linear fit around the designated peak. Afterwards, the error for the number of photons was derived from the backgrounded corrected counts under the peak. When calculating the error for the number of photons per proton per cm depth with the differential method, see (2), the absolute errors of the number of photons detected in each measurement add up:

$$\Delta y_i = \Delta x_i + \Delta x_{i-1} \tag{6}$$

3. Results

This section presents the results of ten irradiations with protons, which were executed to determine the prompt γ-ray yield, the corresponding energy spectra and depth distribution. The measurements are summarized in table 1. The proton beam current was kept stable for each measurement. The live charge counter was used to calculate the effective number of protons for each measurement. During the calibration the relative error of the calibration factor was calculated: $\frac{\Delta C}{C} = 1.3\%$. Using error propagation, the total error was determined for all the results as described in the previous section.

The activation of previously irradiated phantom parts mainly produced photon emission of 511 keV which can be neglected. Furthermore, background measurements showed that there were no significant contributions to the photon emissions above an energy of 3 MeV. This motivated the energy window selection from 3 MeV to 7 MeV.

3.1. Yield comparison

In figure 2, a quantitative comparison for the total γ-ray yield (from 3 MeV to 7 MeV) is summarized for all ten irradiations. For the full absorption measurements, the simulation strongly overestimates the photon yield by 37% (PMMA), 38% (PE), 48% (Graphite) and 38% (SB3). Simulations of the sliced PMMA phantoms revealed that, for the irradiation of the 5 cm target, the yield seemed to be reproduced within the error margins. With increasing target thickness,

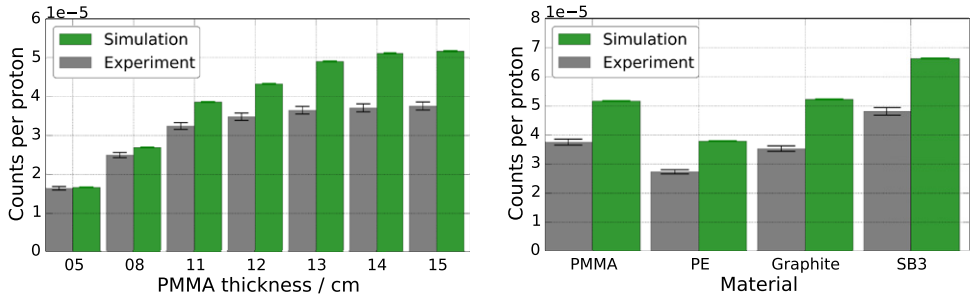

Figure 2. Yield comparison of measured and simulated γ-ray emissions in the energy range from 3 MeV to 7 MeV during multiple irradiations of the *sliced phantom* (left) and full absorption measurements (right) summed over all four Clover channels. The random error (2σ) in the simulated data is barely recognizable. The experimental data also includes the 2σ error from the calibration.

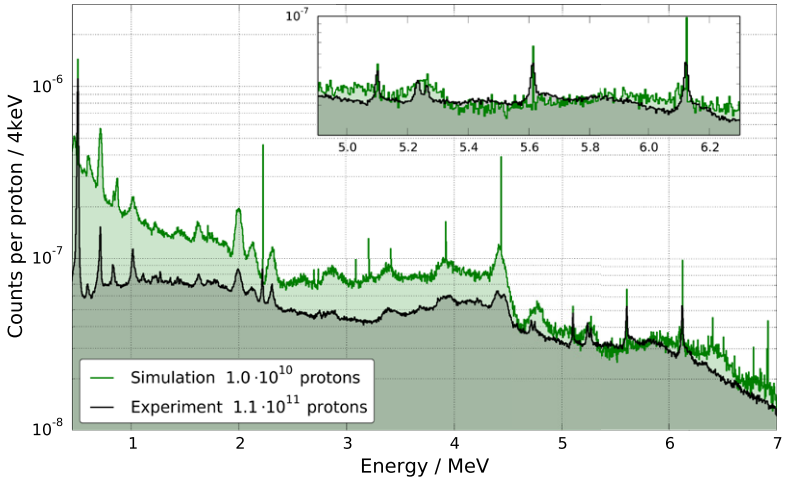

Figure 3. Quantitative comparison of measured and simulated summed γ-ray emission spectrum from about 0.5 MeV–7 MeV for the full absorption PMMA measurement.

the deviations increase up to the values given above. Anyhow, protons which were not completely stopped in the target produced additional γ-ray emissions when hitting objects further downstream such as the beam dump or after scattering in the phantom. So, the simulated yield is also overestimated for these measurements.

3.2. Energy spectrum

When directly looking at the energy spectra, the overestimation of the γ-ray production in the energy range from 3 MeV to 7 MeV can directly be seen. Figure 3 depicts a quantitative comparison of the photon spectra detected during the full absorption PMMA measurement and the corresponding simulation. The production rates for photons of the continuous background in the simulations are higher for almost all energies in the considered interval, except that from about 4 MeV–6 MeV, the baseline is close to the measured one. Despite the consistent overestimation of the continuous background, the overall structure of the measured spectrum was reproduced quite well. Counterparts to all major peaks could be found in the simulated

Table 2. Measured and simulated γ-ray peak intensities with the corresponding background fit interval for the full absorption PMMA measurement.

			Simulation	Experiment
			Counts per proton	
Peaks	E_γ MeV	Interval MeV	10^{-7}	10^{-7}
^{11}C	2.000	1.95 … 2.05	13.58 ± 0.23	3.09 ± 0.11
Neutron capture H	2.225	2.20 … 2.25	2.27 ± 0.10	1.12 ± 0.05
^{12}C and ^{11}B peak	4.439	4.35 … 4.52	23.30 ± 0.30	8.41 ± 0.27
^{12}C and ^{11}B plateau	4.439	3.25 … 4.60	89.71 ± 0.60	40.14 ± 1.16
^{16}O	6.130	6.07 … 6.15	1.20 ± 0.07	1.30 ± 0.06

Note: Listed are the integrals in the summed spectra in the given energy interval. The error consists of the 2σ random error and the contribution of the calibration to the error of the experimental data.

spectrum. Even smaller structures emerging from neutron capture in the Ge crystals were recognized. Furthermore, differences in peak to background intensities were qualitatively reproduced by the simulations, such as the missing neutron capture peak of hydrogen in the graphite spectrum and the missing oxygen peaks in the graphite and PE measurements. Also, the differences in intensity of the ^{12}C plateaus depending on the carbon abundance in the corresponding phantom material could be observed.

In addition to the integral yield comparison, several discrete peaks and energy intervals were also analyzed. A summary is given in table 2. The yields of the γ-ray emissions originating from the ^{11}C 2.00 MeV de-excitation and the neutron capture peak were strongly overestimated by the simulations by a factor of 4.4 and 2.0, respectively. Also, the 4.44 MeV plateau (included the single and double escape peaks and the corresponding Compton continuum) was overestimated by a factor of 2.2. Only the yield of the 6.13 MeV γ-rays from ^{16}O was correctly reproduced within the error margins.

Currently, the implementation of Doppler broadening is very limited in Geant4. A sharp proportion on top of the Doppler-broadened 4.44 MeV peak was observed in the simulations (see figure 3). A process dependent analysis of the prompt γ-rays revealed, that photons emitted at the end of an inelastic proton reaction are broadened and those being created by an inelastic neutron reaction are not.

3.3. Depth profile

To extract the depth profile of the prompt γ-ray emissions from the *sliced phantom* measurements, the differential approach described in the previous section was chosen. Profiles for γ-rays from the ^{11}C de-excitation and neutron capture of hydrogen could not be acquired, since the statistical fluctuation in this energy region (up to about 2 MeV), especially for the thinner targets were too large. Figure 4 presents the resulting DGPs of photons from the 4.44 MeV and 6.13 MeV peak. Measurement $i = 4$ was not completed and could only partially be restored. Therefore, it was left out in the differential analysis and measurement $i = 5$ was treated as an additional slab of 2 cm. Similarly, the DGP for the ^{12}C plateau was determined. Simulations and experiment showed comparable properties as compared to the ^{12}C peak.

The experimentally obtained depth profile for γ-rays from the ^{12}C peak (4.439 MeV) exhibited a plateau and a small peak about 1 cm in front of the Bragg-peak. The peak-to-plateau

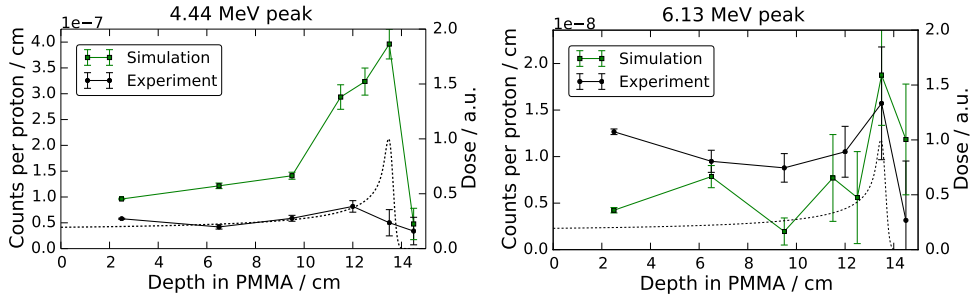

Figure 4. Prompt γ-ray depth profiles for different energy intervals. For both plots, the random errors and for the experimental data the systematic errors are depicted. The dashed line indicates the proton depth dose profile (DDP).

ratio is about 2 : 1. In the simulations, the position of the DGP peak is also in front of the Bragg-peak but the peak-to-plateau ratio is much larger, namely about 3 : 1. Also the difference in total yield is also clearly visible, as already shown in table 2.

The DGP of γ-rays coming from the ^{16}O de-excitation at 6.130 MeV agrees much better with the simulations. The position of the peak at the distal edge is closer to the Bragg-peak. Only the peak-to-plateau ratio seems a little bit larger in the simulations.

In both cases, the first measurement seems to significantly overestimate the plateau. In this case, the protons passing the phantom carry the highest residual energy and the contribution of additional photons which do not emerge from the phantom is also higher as compared to later measurements.

4. Discussion

In this work, a quantitative characterization of prompt γ-ray emissions during proton irradiation of different phantom materials and a comparison with Geant4 MC simulations was performed. The selection of multiple targets made of elements which occur in organic tissue makes the transition to clinical application possible. The total photon yield, the energy spectra and the DGP were successfully assessed, utilizing a conventional HPGe detector system. The latter was evaluated with a novel measurement technique (the *sliced phantom*) which was devised to determine a depth distribution of prompt γ-rays with any conventional detector system, even if direct spatial information of the detected photons is not provided.

Investigation showed that the MC code Geant4 (using the reference physics list QGSP_BIC_HP), in general, overestimates the photon production from nuclear processes (inelastic proton and neutron reactions). Not only the continuous background but also the γ-ray yield for specific processes is too high. The total yield of the photons with an energy from 3 MeV to 7 MeV is up to 50% higher compared to the findings of the experiment. The overall shape of the spectrum in this energy range is reproduced quite well in the simulations. Even smaller peaks are recognizable even though the quantitative yield does not match in all investigated cases. The experimentally determined DGPs are similar to those found during the measurements with a collimated system. Verburg *et al* also observed the peak-to-plateau ratio of the 4.44 MeV photons to be 2 : 1 (Verburg *et al* 2013). This agrees nicely with the results of this work. Corresponding MC simulations yielded a much more distinct peak and an increased peak-to-plateau ratio as compared to the experimental findings.

Verburg reported that the total non-elastic proton cross sections (e.g. $p + {}^{12}$C, $p + {}^{16}$O) are implemented in Geant4 with agreement to the experimental data. The 4.44 MeV γ-ray

production cross section ($^{12}C(p, p')\,^{12}C^{*4.439} + {}^{12}C(p, 2p)^{11}B^{*4.445}$) agrees with the experimental data for proton energies below 10 MeV. For higher energies, it is underestimated by a factor of about two (Verburg *et al* 2012). Therefore, it is fair to assume that the incorrect nuclear de-excitation handling is partly due to the inaccurate overestimation of the γ-ray production. In Geant4, this is executed by the corresponding class files and a database which uses the Evaluated Nuclear Structure Data File (ENSDF) provided by the Lawrence Berkeley National Laboratory (LBNL) Isotope Project. Additionally, the Geant4 nuclear event generators are approximate phenomenological models, which cannot be expected to fully reproduce experimental results. Further investigations would go well beyond the scope of this work.

To improve the resolution of the measured DGPs, the number of slices has to be increased while lowering the slice thickness. This can easily be achieved and offers a fast and reliable method to investigate depth profiles with conventional detectors. Utilizing the accelerator's RF signal, one could use timing information to reduce background during the sliced phantom measurements when the protons are not completely stopped.

The gathered γ-ray emission yield data (from both experiment and simulation) is an important step in understanding the secondary radiation field during proton irradiation. It will benefit the hardware development towards imaging modalities for *in vivo* range verification and dosimetry during particle therapy.

Acknowledgments

This work was supported by the ENVISION project (grant agreement number 241 851). The beam time at KVI-CART, Groningen was provided within the IA-ENSAR project (contract no. RII3-CT-2010-262010). Both were funded by the European Commission within the Seventh Framework Program (FP7).

The authors like to thank Dr R Schwengner from the Nuclear Physics division of the Institute of Radiation Physics at the Helmholtz-Zentrum Dresden-Rossendorf for his valuable advices.

References

Agostinelli S *et al* 2003 Geant4—a simulation toolkit *Nucl. Instrum. Methods Phys. Res.* A **506** 250–303

Duchêne G, Beck F, Twin P, de France G, Curien D, Han L, Beausang C, Bentley M, Nolan P and Simpson J 1999 The clover: a new generation of composite ge detectors *Nucl. Instrum. Methods Phys. Res.* A **432** 90–110

Elekes Z, Belgya T, Molnár G L, Kiss Á Z, Csatlós M, Gulyás J, Krasznahorkay A and Máté Z 2003 Absolute full-energy peak efficiency calibration of a clover–bgo detector system *Nucl. Instrum. Methods Phys. Res.* A **503** 580–8

Enghardt W, Crespo P, Fiedler F, Hinz R, Parodi K, Pawelke J and Pönisch F 2004 Charged hadron tumour therapy monitoring by means of PET *Nucl. Instrum. Methods Phys. Res.* A **525** 284–8

Fiedler F, Kunath D, Priegnitz M and Enghardt W 2012 *Ion Beam Therapy (Biological and Medical Physics, Biomedical Engineering vol 320)* ed U Linz (Berlin: Springer) pp 527–43

Golnik C *et al* 2014 Range assessment in particle therapy based on prompt gamma-ray timing measurements *Phys. Med. Biol.* **59** 5399

Jarlskog C and Paganetti H 2008 Physics settings for using the Geant4 toolkit in proton therapy *IEEE Trans. Nucl. Sci.* **55** 1018–25

Knopf A C and Lomax A 2013 *In vivo* proton range verification: a review *Phys. Med. Biol.* **58** R131

Kormoll T, Fiedler F, Schöne S, Wüstemann J, Zuber K and Enghardt W 2011 A compton imager for *in-vivo* dosimetry of proton beams–a design study *Nucl. Instrum. Methods Phys. Res.* A **626** 114–9

Min C H, Kim C H, Youn M Y and Kim J W 2006 Prompt gamma measurements for locating the dose falloff region in the proton therapy *Appl. Phys. Lett.* **89** 183517

Paans A and Schippers J 1992 Proton therapy in combination with PET as monitor: a feasibility study *Conf. Record of the 1992 IEEE Nuclear Science Symp. and Medical Imaging Conf.* vol 2 pp 957–9

Parodi K *et al* 2007 Patient study of *in vivo* verification of beam delivery and range, using positron emission tomography and computed tomography imaging after proton therapy *Int. J. Radiat. Oncol. Biol. Phys.* **68** 920–34

van der Graaf E, Ostendorf R, van Goethem M J, Kiewiet H, Hofstee M and Brandenburg S 2009 AGORFIRM, the AGOR facility for irradiations of materials *European Conf. on Radiation and Its Effects on Components and Systems* (*RADECS*) pp 451–4

Verburg J M, Riley K, Bortfeld T and Seco J 2013 Energy- and time-resolved detection of prompt gamma-rays for proton range verification *Phys. Med. Biol.* **58** L37

Verburg J M, Shih H A and Seco J 2012 Simulation of prompt gamma-ray emission during proton radiotherapy *Phys. Med. Biol.* **57** 5459